Eigenvalue Problems in Surface Acoustic Wave Filter Simulations

Sabine Zaglmayr[1], Joachim Schöberl[2], and Ulrich Langer[3]

[1] FWF-Start Project Y-192 "3D hp-Finite Elements", Johannes Kepler University Linz, Altenbergerstraße 69, 4040 Linz, Austria `sz@jku.at`
[2] Radon Institute for Computational and Applied Mathematics (RICAM), Altenbergerstraße 69, 4040 Linz, Austria `joachim.schoeberl@oeaw.ac.at`
[3] Institute of Computational Mathematics, Johannes Kepler University Linz, Altenbergerstraße 69, 4040 Linz, Austria `ulanger@numa.uni-linz.ac.at`

Summary. Surface acoustic wave filters are widely used for frequency filtering in telecommunications. These devices mainly consist of a piezoelectric substrate with periodically arranged electrodes on the surface. The periodic structure of the electrodes subdivides the frequency domain into stop-bands and pass-bands. This means only piezoelectric waves excited at frequencies belonging to the pass-band-region can pass the devices undamped.

The goal of the work presented is the numerical calculation of so-called "dispersion diagrams", the relation between excitation frequency and a complex propagation parameter. The latter describes damping factor and phase shift per electrode.

The mathematical model is governed by two main issues, the underlying periodic structure and the indefinite coupled field problem due to piezoelectric material equations. Applying Bloch-Floquet theory for infinite periodic geometries yields a unit-cell problem with quasi-periodic boundary conditions. We present two formulations for a frequency-dependent eigenvalue problem describing the dispersion relation.

Reducing the unit-cell problem only to unknowns on the periodic boundary results in a small-sized quadratic eigenvalue problem which is solved by QZ-methods. The second method leads to a large-scaled generalized non-Hermitian eigenvalue problem which is solved by Arnoldi methods.

The effect of periodic perturbations in the underlying geometry is confirmed by numerical experiments. Moreover, we present simulations of high frequency SAW-filter structures as used in TV-sets and mobile phones.

Key words: piezoelectric effect, periodic structures, Bloch theory, eigenvalue problems

1 Introduction

This work deals with mathematical modeling and numerical simulation of periodic piezoelectric Surface Acoustic Wave filters (briefly SAW-filters) and

results in the computation of so-called "dispersion diagrams". We focus on surface acoustic wave devices used for frequency filtering in wireless communication such as standard components in TV-sets and cellular phones. However, there are many other application fields of SAW-devices as in radar and sensor technology and non-destructive measurement.

A SAW filter consists of a piezoelectric substrate onto whose surface electrode structures are evaporated. We want to concentrate on analyzing frequency filtering effects caused by the periodic arrangement of the electrodes. In practical periodic SAW-filters one arranges some hundreds up to some thousands of electrodes periodically in order to gain the so-called stop-band phenomena. The nature of periodic structures prohibits the propagation of SAWs excited in several frequency ranges. The frequency domain is classified into pass-bands, i.e. frequencies for which excited surface waves get through the periodic piezoelectric device, and stop-bands, i.e. frequencies which cannot pass trough. Therefore, the piezoelectric device can be used for frequency filtering.

A fundamental and recommendable introduction to acoustic field problems, various (surface) wave modes and piezoelectricity is provided by Auld in [3]. The numerical solution of piezoelectric systems via the Finite Element Method is treated e.g. by Lerch in [16]. An overview of the historical development of SAW-devices is given in [19]. The principles of periodic SAW-devices are treated in some IEEE papers like [12], however, in most of them only pure-propagating modes are simulated.

The mathematical justification for the quasi-periodic field distribution is given by Bloch-Floquet theory, which analyzes the spectral properties of ordinary and partial differential operators on periodic structures. This theory was developed by Bloch for solving special problems in quantum mechanics, where one deals with periodic Schrödinger operators, and by Floquet for ordinary differential equations. A description by physicists can be found in Madelung [17] and in Ashcroft and Mehrmann [2]. A functional analytic approach is provided by Simon and Reed [20]. The generalization to partial differential equations with periodic coefficients was done by Bensoussan, Lions and Papanicolaou in [6] for real and elliptic problems and by Kuchment [13], who applied the theory to scalar equations on photonic and acoustic band-gap devices in [4].

Bloch-Floquet theory states that the solution on periodic structures can be decomposed into quasi-periodic functions, so-called Bloch waves. Therefore the problem can be restricted to the unit-cell, i.e. the domain including one electrode. Successive arrangement of this unit-cell yields the original geometry. In order to describe the original periodic system, appropriate quasi-periodic boundary conditions have to be established.

The unit-cell problem turns out to be a coupled-field eigenvalue problem depending on either the frequency or the complex propagation constant. The numerical solution requires discretization, which is done by the Finite Ele-

ment Method (FEM), and the application of an eigenvalue solver. We introduce step-by-step the mathematical tools for handling periodic structures, i.e. formulating and incorporating appropriate boundary conditions and corresponding discretization methods.

We begin with the scalar wave problem and establish three different solution methods for computing the dispersion diagram. All these methods result in non-Hermitian eigenvalue problems of linear or quadratic form. Applying the established methods to periodic structures on piezoelectric problems is formally equivalent to the scalar wave model problem. However, the matrices get indefinite and worse conditioned due to piezoelectric properties, which requires special numerical treatment. Mathematical modeling results in two reasonable versions of frequency-dependent eigenvalue problems, one of quadratic form and the other one of generalized linear form. This requires special theory and numerics of algebraic eigenvalue problems.

In [5] a recommendable collection of state-of-the-art direct and iterative methods for large-scale eigenvalue problems is given. The book includes improved algorithms and implementational details. Tisseur [23] specializes on quadratic eigenvalue problems and Lehouqh [14] on Arnoldi and Implicit Restarted Arnoldi Methods (IRAM). A collection of structure-preserving methods is provided in [8].

The stated eigenvalue problems are solved numerically by our open-source high-order Finite Element solver NGSolve [22] in combination with the mesh generator Netgen [21]. For solving the occurring eigenvalue problems we link the software packages LAPACK [1], providing direct methods, and ARPACK [9], providing Implicit Restarted Arnoldi methods.

The main goal of this paper is the detailed derivation of a mathematical model for surface wave propagation in periodic piezoelectric structures including numerical solution methods and simulation of practical filter structures. The paper is organized as follows. We start with the technical details of surface acoustic wave filters including some first model assumptions, which are based on physical considerations, in Section 2. An introduction to piezoelectric equations is given in Section 3. To gain a detailed mathematical modeling we treat the two main subproblems separately, those are wave propagation in periodic media and the piezoelectric coupled field problem. In Section 4 we derive mathematical tools and solution strategies for the dispersion context of a scalar model problem with periodic coefficients. Section 5 starts with mathematical tools for the piezoelectric coupled field equations and results in combining the solution methods derived in 4 to piezoelectric equations. Numerical results are presented in Section 6. First, the effect of periodic perturbations in the underlying geometry is confirmed. Secondly, we present simulations of a high frequency SAW-filter structures as used in TV-sets or GSM-mobile phones.

2 Problem description and first model assumptions

2.1 Surface acoustic wave filters

We study a piezoelectric *surface acoustic wave* (*SAW, Rayleigh-wave*) device as used for frequency filtering in telecommunications. The main components of such devices are a piezoelectric substrate and two interdigital transducers (IDT) (see Figure 1). Such an IDT is a comb of electrodes evaporated on the top surface of the piezoelectric crystal. Due to the underlying piezoelectric substrate an IDT transforms an alternating voltage into mechanical deformations. An acoustic wave can be excited. Vice versa, mechanical vibrations of the substrate evoke surface charges on the electrodes. An electric signal can be measured at the receiving IDT.

We focus on periodic SAW-filters where frequency filtering is achieved by peri-

Surface Acoustic Wave (SAW) Filter
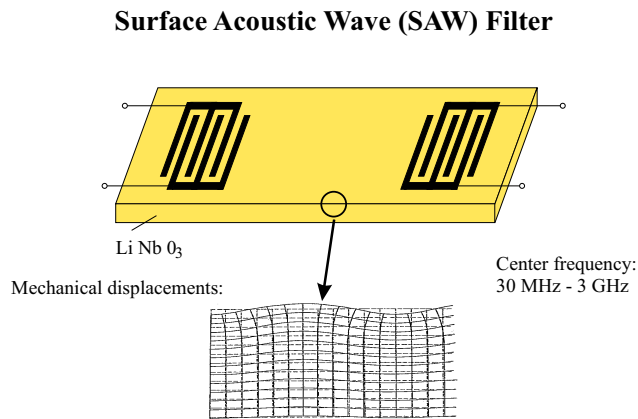
Fig. 1. Principal SAW filter consisting of piezoelectric substrate and input/output IDTs [15]

odic arrangement of electrodes on the surface of the piezoelectric substrate. If an acoustic wave propagates on the surface through the periodic structure, it is partially reflected at each electrode. Depending on the excitation frequency of the acoustic wave the reflected parts interfere constructively or not. If there is huge number of electrodes and the reflections interfere constructively, the wave propagation is prohibited, although the reflections at each electrode are very small. This effect occurs in whole frequency bands, so called band-gaps or stop-bands.

Numerical simulation of the full three-dimensional device is not reasonable. We already perform some model reduction on the geometric domain based on physical considerations: We denote the direction of periodicity by (x_1), the surface normal direction by (x_2) and their perpendicular direction by (x_3).

The dimensional extension of electrodes in (x_3)-direction is huge in comparison to the periodicity. Moreover, we assume homogenous material topology in (x_3)-direction. We are mainly interested in the propagation of Rayleigh-waves and their interaction with the periodic structure. These waves live near the surface, the amplitude decreases rapidly within depth and becomes negligibly small within the depth of a few wavelengths.

In general, surface waves are three-dimensional, but the relevant Rayleigh-waves depend only on the sagittal plane, i.e. the plane spanned by the direction of propagation and the surface normal. Thus, the mechanical and electric fields only depend on x_1 and x_2 coordinates. We can restrict the computational geometry to two dimensions.

In practical SAW devices the IDTs consist of some hundreds up to some thousands of electrodes. Therefore, extending the electrodes periodically to infinity is a suitable approximation.

We choose the infinite 2-dimensional domain which is periodic in x_1-direction to model the piezoelectric substrate with a huge amount of periodically arranged electrodes. See Figure 2.
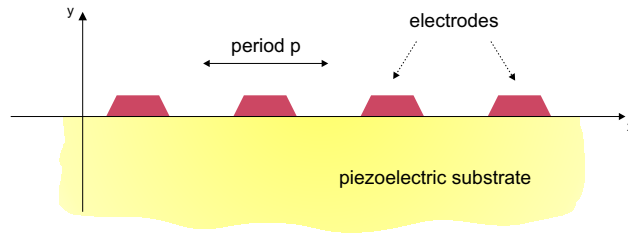
Fig. 2. 2D periodic geometry

2.2 Quasi-periodic wave propagation and the dispersion diagram

As we will see in Section 4.1 and 5.4 the mechanical deformation $u(x,t)$ and the electric potential $\Phi(x,t)$ of surface acoustic waves can be decomposed into Bloch-waves in periodic structrues. These quasi-periodic waves are of the form

$$u(x,t) = e^{i\omega t}e^{(\alpha+i\beta)x}u_p(x), \qquad \Phi(x,t) = e^{i\omega t}e^{(\alpha+i\beta)x}\Phi_p(x)$$

with the p-periodic functions u_p, Φ_p. The wave-propagation can be described by the functional context between the frequency ω and the propagation parameter $\alpha + i\beta$, which is of great interest for engineers designing SAW-filters. The aim of this work is the full calculation of the dispersion diagram, which gives the relation between ω, and the attenuation α and the phase shift β in each periodic cell.

We can observe several wave modes in the dispersion diagram (see Figure 3):
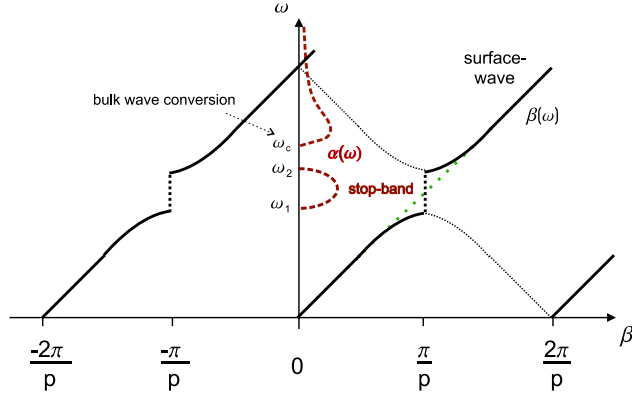
Fig. 3. Dispersion diagram: structure with periodical arranged electrodes

Surface waves belonging to pass- and stop-bands, but also bulk waves which are volume waves. For surface wave propagation the frequency domain is classified in pass-bands and stop-bands as follows:

Wave propagation occurs below the lower stop-band edge ω_1. Surface waves can pass the periodic structure undamped, i.e. they belong to the pass-band. For stop-band frequencies $\omega \in (\omega_1, \omega_2)$ the wave reflections occurring at each electrode, interfere constructively. The wave gets exponentially damped ($\alpha \neq 0$).

Above a certain frequencies ω_c also bulk waves are excited by IDTs. A small damping coefficient α is introduced, by the lack of energy into the material caused by bulk waves. This effect is called "bulk wave conversion" and can only be simulated if the model includes wave absorption of the material.

The green-doted straight line in Figure 3 shows the dispersion context in homogenous materials, where no stop-band effects occur since there are no interfering reflections.

3 The piezoelectric equations

Piezoelectric materials are characterized by the following two effects: The *direct piezoelectric effect* states that a mechanical deformation of a piezoelectric substrate evokes an electric field, which can be measured by charges on the surface. The effect is reversible: A piezoelectric crystal shrinks or stretches, if it is exposed to an electric field (*converse piezoelectric effect*). These phenomena result from special asymmetries occurring in some crystalline materials (e.g. in quartz by nature or in industrial produced ceramics). These effects cannot exist in isotropic media, i.e. piezoelectric materials are always anisotropic. To gain the piezoelectric equations we have to combine electrostatics and elastodynamics. We state the equations in the three-dimensional space.

Elasticity

For an impressed volume force density $f(x)$ the elastic equation of motions states that the mechanical displacement u and the mechanical stresses T are related as

$$\frac{\partial^2 u}{\partial t^2}(x,t) - \mathrm{div}_x T = f(x). \tag{1}$$

The elastic strains S are defined by the geometrical properties

$$S = \frac{1}{2}(\nabla u + (\nabla u)^t). \tag{2}$$

Electrostatics

The electric field intensity E can be expressed by an electric potential Φ as

$$E = -\nabla \Phi. \tag{3}$$

Piezoelectric materials are insulators, i.e. there are no free volume charges. Therefore electrostatics gives

$$-\mathrm{div} D = 0 \tag{4}$$

for the dielectric displacement vector D.

Piezoelectric material laws

We assume a linear piezoelectric coupling of elastic and electric fields, since nonlinear coupling terms are negligibly small. Extending Hook's law and the electrostatic equation for the dielectric displacement by the direct or respectively the converse piezoelectric effect yields

$$\begin{aligned}
T_{ij} &= c_{ijkl} S_{kl} - e_{kij} E_k, \\
D_i &= e_{ijk} S_{jk} + \varepsilon_{ik} E_k,
\end{aligned} \tag{5}$$

where c denotes the mechanical stiffness tensor, ε the dielectric permittivity tensor, e the piezoelectric coupling coefficient tensor.

We point out that the mechanical stiffness matrix and the permittivity matrix are symmetric. Since the direct and converse piezoelectric effect are symmetric, the coupling coefficients are equal for both effects. Due to symmetry considerations we can reduce the four material tensors: c to a 6×6 symmetric matrix, ε to a 3×3 symmetric matrix and e to a 6×3 matrix. We refer the interested reader to [3] for more details on piezoelectric equations.

4 A scalar model problem

To get a better insight into the problem of wave propagation in periodic media and to construct methods for the computation of dispersion diagrams we start with a scalar model problem. We consider the scalar wave equation with periodic coefficients. By the periodic arrangement of the cells $\Omega_k^p = [kp, (k+1)p] \times [0, H]$ we derive the strip $\Omega := \bigcup_{k=-\infty}^{\infty} \Omega_k^p$, which is periodic in (x_1). This will be the underlying geometry modeling the infinite periodic domain. See Figure 4. We search for general solutions $u(x, t)$ of the scalar wave equation

$$
\begin{aligned}
\frac{\partial^2 u}{\partial t^2}(x, t) - \mathrm{div}_x(a(x)\nabla_x u(x, t)) &= 0 \ \text{ on } \Omega, \\
a(x)\frac{\partial u}{\partial n}(x, t) &= 0 \ \text{ on } \Gamma_N, \\
u(x, t) &= 0 \ \text{ on } \Gamma_D.
\end{aligned}
\tag{6}
$$

Since we are interested in the structure of the solution space, we state no initial conditions. The positive coefficient function a describes the periodical properties of the material in x_1-direction, i.e.

$$
a(x_1 + p, x_2) = a(x_1, x_2) \qquad \forall (x_1, x_2) \in \Omega.
\tag{7}
$$

The classical formulation requires higher regularity on the coefficients and on the solutions. With regard to the weak formulation derived later we assume the periodic coefficient a to be positive and piecewise constant. Moreover, the arrangement of Γ_N and Γ_D is assumed to coincide with the periodic nature of the domain, as shown in Figure 4. Note that we state no radiation conditions in x_1-direction.

We can separate the time-dependency by shifting the problem to the fre-
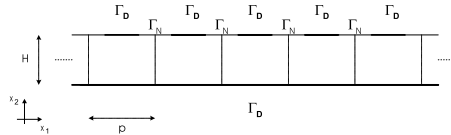
Fig. 4. Infinite periodical cluster 2D (Ω)

quency domain. Therefore, we apply the *time-harmonic ansatz*

$$
\hat{u}(x, t) = \hat{u}(x)\, e^{i\omega t}.
\tag{8}
$$

Form now on we suppress the hat-marker for the complex function $\hat{u}(x) \equiv u(x)$ and agree that to obtain physical results we have to consider the real parts afterwards. The wave-equation (6) transforms to the following eigenvalue problem with periodic-coefficient $a(.)$:

Find the complex-valued eigensolutions u and eigenvalues $\omega \geq 0$ of

$$
-\mathrm{div}(a(x)\nabla u(x)) = \omega^2 u(x) \quad \forall x \in \Omega.
\tag{9}
$$

4.1 Bloch's theorem and the quasi-periodic unit-cell problem

The problem above states an eigenvalue problem with periodic coefficients in an unbounded domain. Bloch-Floquet theory deals with the analysis of partial differential operators with periodic coefficients.

Bloch-theorem on the spectra of periodic operators
We assume the Hermitian partial differential operator
$A : C^2(\Omega, \mathbb{C}) \to C(\Omega, \mathbb{C})$ *to be invariant w.r.t. translations T_p of length p in x_1-direction, i.e.*

$$T_p A = A T_p \quad with \quad T_p : f(.,.) \quad \to \quad f(.+p,.).$$

For every m-dimensional eigenspace $\mathcal{E}_A(\lambda) := \{v \mid Av = \lambda v\}$, there exists a set of **Bloch waves** $(\varphi_i)_{1 \le i \le m}$ *spanning $\mathcal{E}_A(\lambda)$, i.e. satisfying*

$$A\varphi_j = \lambda\varphi_j \ \ and \ \exists \alpha_j, \beta_j \in \mathbb{R} : \ T_p\varphi_j = e^{(\alpha_j + i\beta_j)p}\varphi_j. \tag{10}$$

Lions [6] deals with elliptic operators, but restricts the solution space to the case $\alpha = 0$. The general case is treated in Kuchment [13].

Our problem requires the calculation of Bloch waves solving (9), which are assumed to be *quasi-periodic* in x_1-direction,

$$\exists \alpha, \beta \in \mathbb{R} \, \forall (x_1, x_2) \in \Omega \, : \, u(x_1, x_2) = u_p(x_1, x_2)e^{(\alpha + i\beta)x_1} \tag{11}$$

with u_p being periodic, i.e. $u_p(x_1 + p, x_2) = u_p(x_1, x_2) \ \forall (x_1, x_2) \in \Omega$, or equivalently

$$\exists \alpha, \beta \in \mathbb{R} \, \forall (x_1, x_2) \in \Omega \, : \, u(x_1 + p, x_2) = u(x_1, x_2)e^{i(\alpha + i\beta)p}. \tag{12}$$

Apparently quasi-periodic Bloch waves are fully described by

- a periodic function $u_p(\cdot)$,
- the complex propagation constants $\alpha + i\beta$.

Bloch's theorem justifies a reduction of the infinite problem to one single cell. We choose Ω_0^p and refer to the quasi-periodicity of the Bloch-waves by introducing quasi-periodic boundary conditions on the interfaces $\Gamma_L = \partial\Omega_{-1}^p \cap \partial\Omega_0^p$, $\Gamma_R = \partial\Omega_0^p \cap \partial\Omega_1^p$.

We state the **quasi-periodic unit-cell problem** in strong form as

$$-\mathrm{div}(a\nabla u) = \omega^2 u \quad \text{in } \Omega_0^p \tag{13}$$

$$u = 0 \quad \text{on } \Gamma_{0,D} \tag{14}$$

$$a\frac{\partial u}{\partial n} = 0 \quad \text{on } \Gamma_{0,N} \tag{15}$$

$$\gamma\, u(x_1, x_2) = u(x_1 + p, x_2) \quad \text{for } (x_1, x_2) \in \Gamma_L \tag{16}$$

$$-\gamma\, a(x_1, x_2)\frac{\partial u}{\partial n_l}(x_1, x_2) = a(x_1 + p, x_2)\frac{\partial u}{\partial n_r}(x_1 + p, x_2) \tag{17}$$

$$\text{for } (x_1, x_2) \in \Gamma_L,$$

where $\gamma := e^{(\alpha + i\beta)p}$ and n_l, n_r denote the outer normal vectors on Γ_L and Γ_R, respectively.

4.2 The mixed variational formulation

The variational formulation includes the real-valued or complex-valued Sobolev-spaces
$H^1(\Omega_0^p) := \{u \mid \int_{\Omega_0^p} |u|^2 \, dx + \int_{\Omega_0^p} |\nabla u|^2 \, dx < \infty\}$ and
$H^1_{0,D}(\Omega_0^p) := \{u \in H^1(\Omega_0^p) \mid u = 0 \text{ on } \Gamma_D\}$.
The weak formulation of (13)-(15) in $H^1_{0,D}$ gives

$$\int_{\Omega_0^p} \nabla u \nabla v \, dx - \omega^2 \int_{\Omega_0^p} uv \, dx + \int_{\Gamma_L} a \frac{\partial u}{\partial n} v \, ds + \int_{\Gamma_R} a \frac{\partial u}{\partial n} v \, ds = 0,$$

where we assume $a \in L_\infty(\Omega_0^p)$. The incorporation of the quasi-periodic boundary conditions (16)–(17) is done by a mixed formulation. First, we identify Γ_R and Γ_L by a reference boundary Γ. Secondly, we define the trace-operators for the restriction of left and right boundary, but with respect to the reference boundary Γ, especially the superposition of the trace operator on Γ_l or Γ_r and the identification of the boundaries with Γ:

$$tr_l : H^1(\Omega) \to H^{\frac{1}{2}}(\Gamma), \quad tr_r : H^1(\Omega) \to H^{\frac{1}{2}}(\Gamma)$$
$$u \quad \mapsto \quad u_l \qquad\qquad u \quad \mapsto \quad u_r$$

Thirdly, by introducing a new unknown for the normal-derivative with respect to Γ

$$\lambda := a \frac{\partial u}{\partial n_l} \ \in H^{-\frac{1}{2}}(\Gamma)$$

we can reformulate the weak formulation of (13)–(17) as non-symmetric **mixed variational formulation on the unit cell**:
Find (u, λ) in $H^1(\Omega) \times H^{-\frac{1}{2}}(\Gamma)$ such that

$$\int_{\Omega_0^p} a \nabla u \nabla v \, dx - \omega^2 \int_{\Omega_0^p} uv \, dx + < tr_l v - \gamma \, tr_r v, \lambda > = 0 \quad \forall v \in H^1(\Omega),$$
$$< tr_r u - \gamma \, tr_l u, \mu > \qquad\qquad = 0 \ \forall \mu \in H^{-\frac{1}{2}}(\Gamma). \tag{18}$$

We used the duality product on Γ denoted by $< ., . > := < ., . >_{H^{\frac{1}{2}}(\Gamma) \times H^{-\frac{1}{2}}(\Gamma)}$.
For regular functions this coincides with the L_2-inner-product.
The normal derivative λ takes the role of a *Lagrange-parameter*.

4.3 The frequency-dependent eigenvalue problem

In the mixed variational problem (18) we are interested in possible solutions (u, λ) in combination with the parameter-dependence on ω and γ. There are two possibilities to extract a parameter-dependent eigenvalue problem :

1. *Find all eigensolutions (u, λ) of (18) with positive eigenvalues ω^2 depending on the parameter γ. If we want to calculate the whole dispersion context, the EVP has to be stated depending on a complex parameter $(\alpha + i\beta)$, i.e. two real parameters. This approach is suitable if we state the problem only for pass-bands i.e. $\gamma = e^{i\beta}$.*
2. *Find all eigensolutions (u, λ) of (18) with eigenvalues $\gamma \in \mathbb{C}$ depending on the real-valued frequency ω.* Since we are interested in general complex-propagation parameters $\alpha + i\beta$, we choose this frequency-dependent approach.

Defining the frequency-dependent bilinear form

$$k_\omega(u, v) := \int_{\Omega_0^p} a\nabla u \nabla v \, dx - \omega^2 \int_{\Omega_0^p} uv \, dx, \tag{19}$$

we get an **abstract version of the non-symmetric frequency-dependent eigenvalue-problem** for the quasi-periodic unit-cell problem:

Find eigenfunctions $(u, \lambda) \in H_{0,D}^1(\Omega_p^p) \times H^{-\frac{1}{2}}(\Gamma)$ referring to the eigenvalue $\gamma \in \mathbb{C}$

$$
\begin{aligned}
k_\omega(u, v) \qquad\quad + <(tr_l - \gamma\, tr_r)v, \lambda> &= 0 \quad \forall v \in H_{0,D}^1(\Omega_0^p) \\
<(tr_r - \gamma tr_l)u, \mu> \qquad\qquad\qquad &= 0 \quad \forall \mu \in H^{-\frac{1}{2}}(\Gamma)
\end{aligned}
\tag{20}
$$

dependent on the frequency $\omega \in \mathbb{R}^+$.

4.4 Galerkin-discretization of the frequency-dependent EVP

We assume a Galerkin-discretization $V_h \subset H_{0,D}^1(\Omega_0^p)$ by H^1-conforming Finite Elements. The choice of a Finite Element base for $H^{-\frac{1}{2}}(\Gamma)$ is more challenging. If we consider a general discretization of the right and the left boundary we are faced with the discretization of the dual space for the Lagrange-multiplier. This can be done by Mortar Finite Elements as suggested in [24], [7].

If we use periodic meshes, in the sense that the left and the right boundary are discretized equivalently, we can avoid the assembling of the FE-space for the Lagrange-parameter and simply use nodal constraints on the boundary. In that case, the degrees of freedom are directly connected and so the discrete matrices of the trace-operators are simply identity matrices.

We define the discretized system matrix $K_\omega := [K_{\omega,jk}] == [k_\omega(\varphi_k, \varphi_j)]$ for an H^1-conforming Finite Element base $\{\varphi_j\}$ spanning V_h. The FE-discretization of (20) reads as

$$\begin{pmatrix} K_\omega & Tr_l^t \\ Tr_r & 0 \end{pmatrix} \begin{pmatrix} u_h \\ \lambda_h \end{pmatrix} = \gamma \begin{pmatrix} 0 & Tr_r^t \\ Tr_l & 0 \end{pmatrix} \begin{pmatrix} u_h \\ \lambda_h \end{pmatrix}. \tag{21}$$

We classify the degrees of freedom corresponding to the left (l), the right (r) boundary, and the remaining ones ("inner" dofs, i). The dimensions $n_l = n_r$,

n_i are defined coinciding with this classification and $\dim(V_h) =: n = n_i + 2 \cdot n_l$. Considering the sparsity and the symmetry of the FE-matrices we arrive at a **parameter-dependent discretized generalized eigenvalue-system** of the following structure:

$$
\begin{pmatrix}
K_{\omega,ii} & K_{\omega,li}^T & K_{\omega,ri}^T & 0 \\
K_{\omega,li} & K_{\omega,ll} & 0 & I \\
K_{\omega,ri} & 0 & K_{\omega,rr} & 0 \\
\hline
0 & 0 & I & 0
\end{pmatrix}
\begin{pmatrix}
u_i \\ u_l \\ u_r \\ \lambda
\end{pmatrix}
= \gamma
\begin{pmatrix}
0 & 0 & 0 & 0 \\
0 & 0 & 0 & 0 \\
0 & 0 & 0 & I \\
\hline
0 & I & 0 & 0
\end{pmatrix}
\begin{pmatrix}
u_i \\ u_l \\ u_r \\ \lambda
\end{pmatrix}.
\tag{22}
$$

Remark 1. The generalized eigenvalue problem $Ax = \gamma Bx$ defined in (22) has the following properties:

1. The right hand side matrix B has a large kernel ($\dim(\ker B) = n_i + n_l$), which corresponds to infinite eigenvalues. There are $n_i + n_l$ infinite and $2n_l$ finite eigenvalues.
2. The eigenvalue-problem is *symplectic*, i.e. if γ is an finite non-zero eigenvalue then $\frac{1}{\gamma}$ is also an eigenvalue. One can exploit and preserve the special structure by using structure-preserving computational methods as proposed by Mehrmann in [18].
3. Concerning dispersion diagrams we are mainly interested in eigenvalues $\gamma = e^{(\alpha+i\beta)p}$ near the unit-circle, i.e. $|\gamma| \approx 1$.

4.5 A model improvement by absorbing boundary conditions

So far we have used standard boundary conditions on the bottom boundary of the cell. Since we are interested in surface effects, we do not want to simulate the whole thickness of the underlying substrate, we cut off the domain a few wavelengths away from the surface. The assumption of Dirichlet or Neumann boundary conditions is not suitable, since these types of artificial boundary introduce unnatural reflections. Moreover, damping effects in surface waves, caused by bulk wave radiation effects, are only possible in models including wave absorption into the substrate. These reflections can be avoided or at least minimized by the choice of absorbing boundary conditions (ABCs).

First order absorbing boundary conditions are introduced by complex-valued frequency-dependent Robin boundary conditions of the form

$$
n^T(a\nabla u) = i\omega u \text{ on } \Gamma_{bot}.
$$

This condition is exact for plane waves in outer normal direction n, but still leads to partial reflections for general plane waves. This approach leads to the complex-symmetric bilinear form

$$
k_\omega^{\mathrm{ABC}}(u, v) := \int_{\Omega_0^p} a\nabla u \nabla v \, dx + i\omega c(u, v) - \omega^2 \int_{\Omega_0^p} uv \, dx
\tag{23}
$$

with $c(u, v) := \int_{\Gamma_{bot}} uv \, ds$.

Quite recently **the method of perfectly matched layers (PML)** became very popular. We do not want to go into a detailed description of this method. In order to construct solution methods which can be also applied to PML boundaries, we only point out its effect on the structure of the corresponding bilinear form k_ω. Technically one introduces an artificial boundary layer in which the coefficients of the underlying PDE are extended into the complex plane. On the infinite level PML perfectly absorbs plane waves in any arbitrary direction. On the discrete level the quality of absorption can be controlled by the choice of the FE-discretization. By this approach the bilinear form extends to

$$k_\omega^{\mathrm{PML}}(u, v) := \int_{\Omega_0^p} \tilde{a} \nabla u \nabla v \, dx - \omega^2 \int_{\Omega_0^p} \tilde{\rho} u v \, dx \qquad (24)$$

with complex-valued parameters $\tilde{a}$ and $\tilde{\rho}$. This bilinear form is again *complex-symmetric*.

Remark 2. By the choice of the proposed ABCs, the system-matrix K_ω in the generalized algebraic EVP (22) gets complex-valued and is complex-symmetric.

4.6 Solution strategies

In this section we want to construct two strategies for the solution of the generalized algebraic EVP (22) for complex-valued and complex-symmetric matrices K_ω.
We state two reduced eigenvalue problems which still have the same finite spectrum as the initial system. This is achieved by reducing infinite eigenvalues resulting from the large kernel of the right-hand-side matrix in (22).

The Inner-Node-Matrix method

We use the classification in inner (i), left (l) and right (r) degrees of freedom. Substituting first $u_r = \gamma u_l$ and then $\lambda = -K_{\omega,li} u_i - K_{\omega,ll} u_l$ leads to a generalized non-Hermitian linear eigenvalue problem of the form

$$\begin{pmatrix} K_{\omega,ii} & K_{\omega,il} \\ K_{\omega,ir}^T & 0 \end{pmatrix} \begin{pmatrix} u_i \\ u_l \end{pmatrix} = \gamma \begin{pmatrix} 0 & -K_{\omega,ir} \\ -K_{\omega,il}^T & -K_{\omega,ll} - K_{\omega,rr} \end{pmatrix} \begin{pmatrix} u_i \\ u_l \end{pmatrix}. \qquad (25)$$

We point out that in the above problem none of the two matrices is regular nor symmetric, but by spectral transformation coinciding with $\mu := \frac{1}{\gamma-1}$ we get the following equivalent problem:

Find eigenvectors $\begin{pmatrix} u_i \\ u_l \end{pmatrix} \in \mathbb{C}^{n_i + n_l}$ w.r.t. the eigenvalues $\mu = \frac{1}{\gamma-1}$:

$$\begin{pmatrix} 0 & -K_{\omega,ir} \\ -K_{\omega,il}^T & -K_{\omega,ll} - K_{\omega,rr} \end{pmatrix} \begin{pmatrix} u_i \\ u_l \end{pmatrix} = \mu \begin{pmatrix} K_{\omega,ii} & K_{\omega,il} + K_{\omega,ir} \\ K_{\omega,ir}^T + K_{\omega,il}^T & K_{\omega,ll} + K_{\omega,rr} \end{pmatrix} \begin{pmatrix} u_i \\ u_l \end{pmatrix}.$$
$$\qquad (26)$$

The right-hand-side matrix is obviously regular and complex-symmetric. Moreover, all involved matrices are sparse.

An implementation of the implicitly restarted Arnoldi-algorithm is provided by the software-package ARPACK. The package includes an iterative solver for generalized non-Hermitian eigenvalue $Av = \gamma Bv$ which only requires matrix-vector products and the application of the inversion. Therefore, the sparsity of the FE-matrices can be exploited. In each frequency step we have to perform a Sparse-Cholesky factorization of B.

The Schur-complement method

We start with the already reduced system stated in (25) and take the Schur-complement with respect to the inner degrees of freedom. We state the Schur-complement of K_ω as

$$S := -\left(K_{\omega,li}, K_{\omega,ri}\right) K_{\omega,ii}^{-1} (K_{il} - \gamma K_{ir}) + \begin{pmatrix} K_{\omega,ll} & 0 \\ 0 & K_{\omega,rr} \end{pmatrix}. \qquad (27)$$

Substituting u_i by $u_i = -K\omega, ii^{-1}(K_{il} - \gamma K_{ir})u_l$ in (25) we result in the following **frequency-dependent quadratic eigenvalue problem**:

Find eigenpairs $(\gamma, u_l) \in \mathbb{C} \times \mathbb{C}^{n_l}$ such that

$$\gamma^2 S_{lr} u_l + \gamma(S_{ll} + S_{rr})u_l + S_{lr}^T u_l = 0. \qquad (28)$$

In each frequency step we first calculate the inverse of the sparse and complex-symmetric matrix $K_{\omega,ii}^{-1}$ by a Sparse-Cholesky-factorization and assemble the Schur-complement. The quadratic eigenvalue problem is tackled by linearization to a double-sized generalized eigenvalue problem, which is solved by the QZ-method implemented in LAPACK.

5 Piezoelectric equations and periodic structures

In this section we want to combine the three main modeling steps,

- the underlying piezoelectric equations, which lead to a coupled field problem of saddle-point structure (indefinite, but symmetric),
- absorbing boundary conditions for acoustic waves in piezoelectric media in order to enable wave absorption of the substrate,
- acoustic wave propagation in periodic structures and its solution strategies.

Here, mathematical modeling, analysis and solution strategies get more technical due to the governing piezoelectric equations. One has to overcome some problems due to the indefinite saddle-point structure of piezoelectric equations. But the quasi-periodic problem results in a formally equivalent eigenvalue problem, which can be solved numerically with the methods introduced above.

5.1 2d geometry and anisotropic materials

At first, we adopt the three-dimensional piezoelectric equations given in (1)–(5) to the fact that surface waves only depend on the sagittal plain. This was the justification to reduce the geometry to the plain spanned up by the direction of surface wave propagation (x_1) and the normal onto the surface (x_2). Due to the anisotropic properties of the material general surface waves can polarize (particle motion) outside the sagittal plane. Even though all field quantities only depend on the (x_1, x_2)-plane, a mechanical deformation in (x_3)-direction is possible. Therefore, the equations for the elastic strain (2) and the electric field (3) simplify to

$$S(u) = \frac{1}{2}\Big(\nabla_{(x_1,x_2,x_3)}u(x_1,x_2) + \big(\nabla_{(x_1,x_2,x_3)}u(x_1,x_2)\big)^t\Big), \qquad (29)$$

$$E = \nabla_{(x_1,x_2,x_3)}\Phi(x_1,x_2) = \left(\frac{\partial \Phi}{\partial x_1}, \frac{\partial \Phi}{\partial x_2}, 0\right)^t. \qquad (30)$$

From now on we denote the equations (1),(29),(3),(29),(4) as the *governing piezoelectric equations for the three-dimensional mechanical displacement $u = (u_1, u_2, u_3)^t$ and the scalar potential Φ.*

5.2 The underlying infinite periodic piezoelectric problem

The cell-based periodic model geometry

The periodic geometry Ω can be described in terms of successive arrangement of a unit-cell Ω_0^p (with $\mathrm{diam}_{x_1}(\Omega_0^p) = p$) of an analogous structure as shown in Figure 5. We denote the translation of this cell parallel to the x_1-axis as the k-th cell $\Omega_k^p := \Omega_k^p := \{y = (k.p, 0) + x | x \in \Omega_0^p\}$ and achieve a representation of an infinite periodic strip Ω by $\Omega := \bigcup_{k=-\infty}^{\infty} \Omega_k^p$.
Each cell basically consists of a piezoelectric substrate $\Omega_{k,S}$ with one evaporated electrode $\Omega_{k,E}$; these two domains are disjoint but matching. In numerical computation we will choose the model geometry shown in Figure 4.
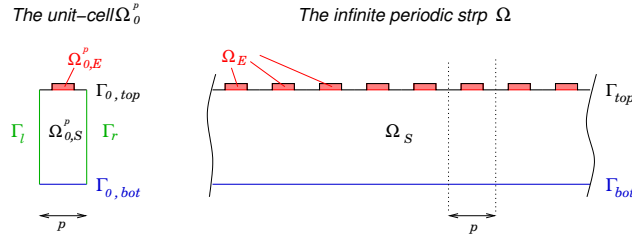
Fig. 5. Underlying cell-based periodic geometry

The piezoelectric equations with periodic coefficients on Ω

Shifted to the frequency domain by a harmonic ansatz, the piezoelectric equations for the mechanical displacement (u_1, u_2, u_3) and the scalar potential Φ are

$$-\text{div}\Big(c : \big(\nabla u + (\nabla u)^t\big) + \epsilon : \nabla\Phi\Big) = \omega^2 \rho u \text{ in } \Omega,$$
$$-\text{div}\Big(e^t : \big(\nabla u + (\nabla u)^t\big) - \varepsilon : \nabla\Phi\Big) = 0 \qquad \text{in } \Omega, \tag{31}$$

with underlying periodic structure Ω and periodic coefficient matrices $T_p c = c, T_p e = e, T_p \rho = \rho$. On the metallic electrodes Ω_E the piezoelectric coupling coefficient e is set to zero. Concerning the boundary conditions we choose homogenous Dirichlet boundary condition for the potential on $\Gamma_E := \partial\Omega \cap \partial\Omega_E =: \Gamma_D$ in order to model short-circuited electrodes. The remaining top-surface boundary is assumed to be charge-free. Concerning the mechanical field the whole top-surface boundary is assumed to be stress-free. Therefore, the following boundary conditions are claimed for (31)

$$\begin{array}{llll}\text{short-circuited electrodes} & \Phi = 0 & \text{on } \Gamma_E := \partial\Omega \cap \partial\Omega_E, \\ \text{stress-free:} & n^t.T = 0 & \text{on } \Gamma_{top}, \\ \text{charge-free:} & n^t.D = 0, & \text{on } \Gamma_{top}\backslash\Gamma_E. \end{array} \tag{32}$$

$$\text{Absorbing BCs on } \Gamma_{bot} \tag{33}$$

with normal stresses $n^t.T := n^t\big(c : \big(\nabla u + (\nabla u)^t\big) + e : \nabla\Phi\big)$
and normal charges $n^t.D := n^t\big(e^t : \big(\nabla u + (\nabla u)^t\big) - \varepsilon : \nabla\Phi\big)$.
Solving the periodic problem again requires the computation of Bloch waves. Therefore, it can be restricted to a piezoelectric unit-cell problem with quasi-periodic boundary conditions for mechanical and electric field quantities. Analogous to the scalar model, we begin with the mathematical tools required for the piezoelectric unit-cell problem with standard-boundary conditions. The incorporation of the quasi-periodicity will be done in the second step.
For sake of simplicity we assume the charge- and stress-free boundary conditions

$$n^t.T = 0, \quad n^t.D = 0 \quad \text{on } \Gamma_{bot} \tag{34}$$

on the bottom boundary in the first stage of modeling.

5.3 Piezoelectric equations in weak and discretized form

Restriction of the time-harmonic piezoelectric equations stated in (31),(32),(34) onto the unit-cell Ω_o^p and its weak formulations yields the following eigenvalue problem:

Find eigensolutions $(u, \Phi) \in \big[H^1(\Omega_0^p)\big]^3 \times H^1_{0,D}(\Omega_0^p)$ corresponding to the eigenvalues ω^2 such that $\forall v \in H^1(\Omega_0^P)^3 := \big[H^1(\Omega_0^P)\big]^3$, $\forall \Psi \in H^1_{0,D}(\Omega_0^p)$

$$\begin{array}{l} \int_{\Omega_0^p}(Bv)^T : c\,Bu \quad + \int_{\Omega_0^p}(S(v))^t : e^t\nabla\Phi\,dx = \omega^2 \int_{\Omega_0^p}\rho\,v^t u\,dx \\ \int_{\Omega_0^p}(\nabla\Psi)^t : e\,Bu\,dx - \quad \int_{\Omega_0^p}(\nabla\Psi)^t\,\varepsilon\,\nabla\Phi\,dx \quad = 0 \end{array} \tag{35}$$

Due to the large kernel in the right hand side the eigenvalue problem is degenerated, which leads to infinite eigenvalues.

For the sake of simplicity we introduce the mechanical bilinear form

$$a_{uu}(u,v) := \int_{\Omega_0^p} S(v)^t : c\, S(u)\, dx,$$

the piezoelectric coupling bilinear forms

$$a_{u\Phi}(u,\Phi) = a_{\Phi u}(\Phi,u) := \int_{\Omega_0^p} S^t(u) : e^t \nabla \Phi\, dx,$$

the dielectric bilinear form

$$a_{\Phi\Phi}(\Phi,\Psi) = \int_{\Omega_0^p} (\nabla \Psi)^t\, \varepsilon\, \nabla \Phi\, dx,$$

and the mechanical mass bilinear form

$$m_{uu}(u,v) := \int_{\Omega_0^p} \rho\, v^t u\, dx.$$

On the structure of piezoelectric discretized eigenvalue-problems

The discretization of $H^1(\Omega_0^p)^3$ and $H^1(\Omega_0^p)$ with conforming Finite Elements yields a algebraic eigenvalue-problem of the special saddle-point structure

$$\begin{pmatrix} A_{uu} & A_{u\Phi} \\ A_{\Phi u} & -A_{\Phi\Phi} \end{pmatrix} \begin{pmatrix} u_h \\ \Phi_h \end{pmatrix} = \omega^2 \begin{pmatrix} M_{uu} & 0 \\ 0 & 0 \end{pmatrix} \begin{pmatrix} u_h \\ \Phi_h \end{pmatrix}. \tag{36}$$

The matrix blocks correspond to the mechanical, dielectric and piezoelectric bilinear forms. Therefore, the problem is symmetric since the sub-matrices satisfy $A_{uu} = A_{uu}^t, A_{\Phi\Phi} = A_{\Phi\Phi}^t, A_{\Phi u} = A_{u\Phi}^t, M_{uu} = M_{uu}^t$. The eigenvalue problem is degenerated. It possesses $dim(\Phi_h)$ infinite eigenvalues.

The Schur-complement with respect to the potential Φ_h yields

$$\left(A_{uu} + A_{u\Phi} A_{\Phi\Phi}^{-1} A_{\Phi u} \right) u_h = \omega^2 M_{uu} u_h,$$

which states a positive-definite eigenvalue problem. However, we will not pursuit this strategy, due to the computational costs for inverting $A_{\Phi\Phi}$.

5.4 The quasi-periodic unit-cell problem

Due to Bloch's theorem (general version stated in [13]) we use Bloch waves

$$\begin{aligned} u(x_1,x_2) &= u_p(x_1,x_2)e^{(\alpha+i\beta)x_1} \quad \text{with } u_p \ \ p-\text{periodic in } x_1 \\ \Phi(x_1,x_2) &= \Phi_p(x_1,x_2)e^{(\alpha+i\beta)x_1} \quad \text{with } \Phi_p \ \ p-\text{periodic in } x_1 \end{aligned}$$

as ansatz for the eigenfunctions in the periodic piezoelectric eigenvalue problem (31)–(32) together with either (33) or (34).

Therefore, **the quasi-periodic unit-cell problem** is stated by (31),(32), and (33) or (34) restricted onto Ω_0^p together with the quasi-periodic boundary conditions

$$\gamma\, u(x_1, x_2) = u(x_1 + p, x_2) \qquad \text{for } (x_1, x_2) \in \Gamma_L,$$
$$-\gamma\, n^t \cdot T(x_1, x_2) = n^t \cdot T(x_1 + p, x_2) \qquad \text{for } (x_1, x_2) \in \Gamma_L,$$
$$\gamma\, \Phi(x_1, x_2) = \Phi(x_1 + p, x_2) \qquad \text{for } (x_1, x_2) \in \Gamma_L,$$
$$-\gamma\, n^t \cdot D(x_1, x_2) = n^t \cdot D(x_1 + p, x_2) \qquad \text{for } (x_1, x_2) \in \Gamma_L,$$

(37)

with $\gamma := e^{(\alpha + i\beta)p}$.

Now, the solution strategy is formally equivalent to that presented for the scalar model problem. We interpret the quasi-periodic unit-cell problem as eigenvalue-problem for the propagation-constant γ while depending on the frequency ω.

We identify the quasi-periodic boundaries Γ_l and Γ_r with a reference boundary Γ. The corresponding trace operators tr_l and tr_r are defined as the composition of the standard H^1-trace operator onto Γ_L and the boundary identification of Γ_l or Γ_r with Γ: $tr_l : H^1 \Omega_p^0 \to H^{\frac{1}{2}}(\Gamma_l) \overset{id}{\to} H^{\frac{1}{2}}(\Gamma)$, and vice versa for tr_r. The trace-operator on the three-dimensional mechanical field u in $H^1(\Omega_0^p)^3$ is defined component-wise as $tr_l u := (tr_l u_1, tr_l u_2, tr_l u_3)$ in $H^{\frac{1}{2}}(\Gamma)^3 := [H^{\frac{1}{2}}(\Gamma)]^3$ Furthermore, by introducing new unknowns for the normal fluxes on the left boundary with respect to Γ

$$\lambda := n^t \cdot T \in H^{-\frac{1}{2}}(\Gamma)^3 \quad \text{and} \quad \zeta := n^t \cdot D \in H^{-\frac{1}{2}}(\Gamma), \tag{38}$$

we result in the **frequency-dependent mixed variational formulation**:

Find eigensolutions $(u, \Phi, \lambda, \zeta)$ corresponding to eigenvalues $\gamma \in \mathbb{C}$ with $(u, \Phi, \lambda, \zeta) \in H^1(\Omega_0^p)^3 \times H^1_{0,D}(\Omega_0^p) \times H^{-\frac{1}{2}}(\Gamma)^3 \times H^{-\frac{1}{2}}(\Gamma)$ such that $\forall v \in H^1(\Omega_0^p)^3, \forall \Psi \in H^1_{0,D}(\Omega_0^p), \forall \mu \in H^{-\frac{1}{2}}(\Gamma)^3, \forall \nu \in H^{-\frac{1}{2}}(\Gamma)$

$$a_{uu}(u,v) + a_{u\Phi}(\Phi, v) - \omega^2 m(u,v) + \, < (tr_l - \gamma\, tr_r)v, \lambda > \, = 0$$
$$a_{\Phi u}(u, \Psi) - a_{\Phi\Phi}(\Phi, \Psi) \qquad\qquad + \, < (tr_l - \gamma\, tr_r)\Psi, \zeta > \, = 0$$
$$< (\gamma\, tr_l - tr_r)u, \mu > \qquad\qquad\qquad\qquad = 0$$
$$< (\gamma\, tr_l - tr_r)\Phi, \nu > \qquad\qquad\qquad\qquad = 0$$

(39)

is satisfied for given parameters ω^2.

The duality-product $< ., . >$ refers to $< ., . >_{H^{\frac{1}{2}}(\Gamma)^3 \times H^{-\frac{1}{2}}(\Gamma)^3}$ or $< ., . >_{H^{\frac{1}{2}}(\Gamma) \times H^{-\frac{1}{2}}(\Gamma)}$ respectively.

Again, the introduced unknowns λ, ζ for the normal fluxes on Γ_l with respect to Γ take the role of **Lagrange-multipliers**.

To gain a compact formalism we use the abbreviations $\tilde{u} := (u, \Phi) \in H^1_{0,D_4}(\Omega_0^p)^4 := H^1(\Omega_0^p)^3 \times H^1_{0,D}(\Omega_0^p)$, and $\tilde{v} := (v, \Psi)$, and on the frequency-dependent piezoelectric bilinear form

$$k^\omega(\tilde{u}, \tilde{v}) := k^\omega\big((u, \Phi), (v, \Psi)\big)$$
$$:= a_{uu}(u, v) + a_{u\Phi}(\Phi, v) - \omega^2 m(u, v) \tag{40}$$
$$+ a_{\Phi u}(u, \Psi) - a_{\Phi\Phi}(\Phi, \Psi).$$

An abstract version of the non-symmetric frequency-dependent eigenvalue problem for the quasi-periodic unit-cell problem can be stated as

Find eigensolutions $(\tilde{u}, \tilde{\lambda}) \in H^1_{0,D}(\Omega_0^p)^4 \times H^{-\frac{1}{2}}(\Gamma)^4$ corresponding to eigenvalues $\gamma \in \mathbb{C}$ such that

$$\begin{aligned} k_\omega(\tilde{u}, \tilde{v}) \qquad &+ < \tilde{\lambda}, (tr_l - \gamma\, tr_r)\tilde{v} > = 0 \ \ \forall \tilde{v} \in H^1(\Omega_0^p)^4 \\ < (\gamma\, tr_l - tr_r)\tilde{u}, \tilde{\mu} > \qquad &= 0 \ \ \forall \tilde{\mu} \in H^{-\frac{1}{2}}(\Gamma)^4 \end{aligned} \tag{41}$$

is satisfied for given parameters ω^2.
The duality-product $< ., . >$ refers to $< ., . >_{H^{\frac{1}{2}}(\Gamma)^4 \times H^{-\frac{1}{2}}(\Gamma)^4}$.

Model extension to absorbing boundary conditions

In case of piezoelectric equations absorbing boundary conditions are a bit challenging. The degeneration of the frequency-dependent eigenvalue problem causes some technical difficulties. However, we only state the formal characteristics of the extended system bilinear forms

$$k_\omega^{\mathrm{ABC}} := a\big((u, \Phi), (v, \Psi)\big) + i\,\omega\, c\big((u, \Phi), (v, \Psi)\big) - \omega^2 m\big((u, \Phi), (v, \Psi)\big), \tag{42}$$
$$k_\omega^{\mathrm{PML}} := \tilde{a}\big((u, \Phi), (v, \Psi)\big) - \omega^2\, \tilde{m}\big((u, \Phi), (v, \Psi)\big). \tag{43}$$

The absorbing bilinear form $c(.,.)$ is positive-definite. The complex-valued PML-bilinear forms $\tilde{a}(.,.)$ and $\tilde{m}(.,.)$ are complex-symmetric.

The discretized eigenvalue problem

Analogous to the scalar case, we assume matching meshes on the left and the right boundary. Therefore, a discretization of $H^{-\frac{1}{2}}(\Gamma)^4$ by Mortar-Elements can be avoided. We can use nodal constraints for the Lagrange-parameter and the discrete trace-operators corresponding to tr_l and tr_r simplify to identity matrices.
Discretization of $H^1_{0,D}(\Omega_0)$ for the frequency-dependent piezoelectric bilinear form is done in the way already described for (36). Galerkin-discretization of (41) leads to **parameter-dependent discretized generalized eigenvalue-system** (compare with (22))

$$\begin{pmatrix} K_{\omega,ii} & K_{\omega,li}^T & K_{\omega,ri}^T & 0 \\ K_{\omega,li} & K_{\omega,ll} & 0 & I \\ K_{\omega,ri} & 0 & K_{\omega,rr} & 0 \\ \hline 0 & 0 & I & 0 \end{pmatrix} \begin{pmatrix} \tilde{u}_i \\ \tilde{u}_l \\ \tilde{u}_r \\ \lambda \end{pmatrix} = \gamma \begin{pmatrix} 0 & 0 & 0 & 0 \\ 0 & 0 & 0 & 0 \\ 0 & 0 & 0 & I \\ \hline 0 & I & 0 & 0 \end{pmatrix} \begin{pmatrix} \tilde{u}_i \\ \tilde{u}_l \\ \tilde{u}_r \\ \lambda \end{pmatrix}, \tag{44}$$

where each $\tilde{v^i}$ refers to 4 degrees of freedom $(u_1^i, u_2^i, u_3^i, \Phi^i)$ and each classified (i, l, r) matrix block is of the following (complex)-symmetric saddle point structure

$$K_{\omega,\alpha,\beta} = \begin{pmatrix} K_{\omega,\alpha,\beta,\,uu} & K_{\omega,\alpha,\beta,\,\Phi u}^T \\ K_{\omega,\alpha,\beta,\,\Phi u} & -K_{\omega,\alpha,\beta,\,\Phi\Phi} \end{pmatrix} \qquad \text{for } \alpha, \beta \in \{i, l, r\}. \qquad (45)$$

Standard boundary conditions on the bottom leads to real-valued matrices, absorbing ones to complex-valued ones. We suppressed the h-subscript denoting the discrete level. Due to the abstract formulation of the scalar and the piezoelectric eigenvalue problem we can apply the solution strategies of the scalar model, i.e. the Inner-Node-Matrix method or the Schur-Complement method in Subsection 4.6.

6 Numerical results

In case of a 2 dimensional geometry the implementation of the Schur-Complement method together with a Sparse-Cholesky-Factorization is suitable. However, if one thinks about simulations on 3 dimensional geometries, one has to perform the Inner-Node-Matrix method.
The Schur-Complement method is implemented in the high order FE-Solver NGSolve [22] using an LAPACK eigenvalue solver (`zgeev, dggev`) [1].

6.1 The scalar model problem

We use the scalar model problem to examine the specific influence of periodic perturbations on surface wave propagation. Therefore, we determine the dispersion context for 3 different problem types based on the geometry shown in Figure 4:

1. Wave propagation in *homogenous media*, where we assume homogenous Neumann BCs on the top and the surface ($\Gamma_D = \emptyset$, $\Gamma_N := \Gamma_{top} \cup \Gamma_{bot}$). See Figure 6.
2. Wave propagation in *periodic media*, where periodic perturbations are simulated by periodically arranged homogenous Dirichlet- and Neumann-BCs on the top surface (see Figure 4). The homogenous Dirichlet conditions is used as imitation of short-circuited electrodes, where a vanishing potential can be assumed. See Figure 7.
3. Wave propagation in *periodic media* with first order *absorbing boundary conditions* on the bottom surface Γ_{bot}. The periodic structure is modeled as described in item 2. See Figure 8.

In the three following dispersion diagrams complex propagation constants which belong to pass-bands are drawn in green, those belonging to stop-bands in red. These diagrams include both bulk waves and surface waves. The classification can be performed by examining the corresponding eigenvectors.
In the homogenous case, there are no stop-bands. We gain pure imaginary propagation constants $i\beta$ corresponding to continuous pass-bands.
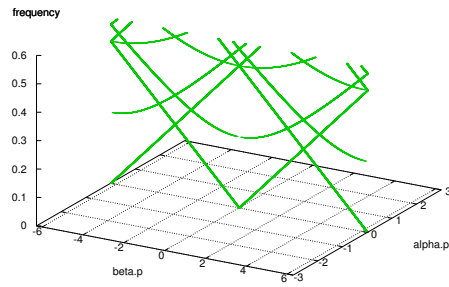
Fig. 6. Scalar model: Dispersion relation in a homogenous structure.
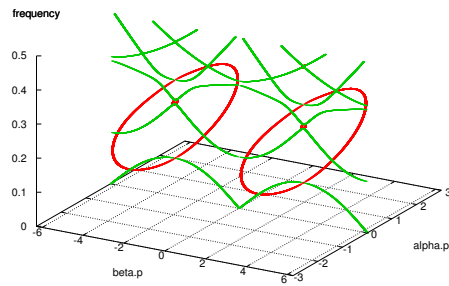
Fig. 7. Scalar model: Dispersion relation in a periodic structure.
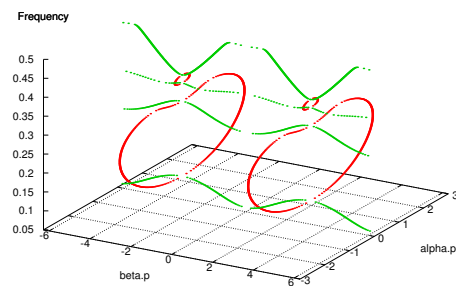
Fig. 8. Scalar model: Dispersion relation in a periodic structure with ABC.

6.2 Simulation of a piezoelectric periodic structure

Since the dispersion diagram gives information on many parameters of wave propagation, which are used in other models and simulations, we want to determine the eigenvalues very accurately. Our main aspects are frequency domains where the dimension of the unit-cell is in the range of half the wavelength. Therefore, higher order polynomials should approximate these waves very accurately even for coarse meshes. However, the entering corners of the electrodes and the jumping coefficients cause singularities in the solution. These singularities cannot be resolved simply by increasing the polynomial order of the ansatz functions, but only by a special local mesh-refinement denoted as *hp-refinement*. Both methods consist of two main steps. First the computation of an inverse (SC-method) or respectively a Sparse-Cholesky decomposition. Secondly, the solution of an eigensystem, here the decrease of degrees of freedom is very important for decreasing computational times.

We simulate the dispersion context of a TV-filter structure as used in practice
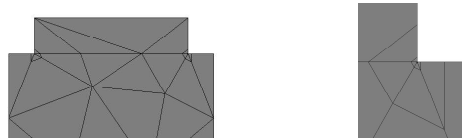
Fig. 9. Special local refinement at singularities

with Lithium-Niobate substrate and aluminum short-circuited electrodes. The topology is chosen as shown in Figure 4. On the bottom first order absorbing boundary conditions are assumed. We used 52 elements of polynomials order $p = 4$ and an hp-refinement of 3 levels, which results in $4 \cdot 609$ degrees of freedom. Figure 10 shows a two-dimensional plot of the dispersion context near
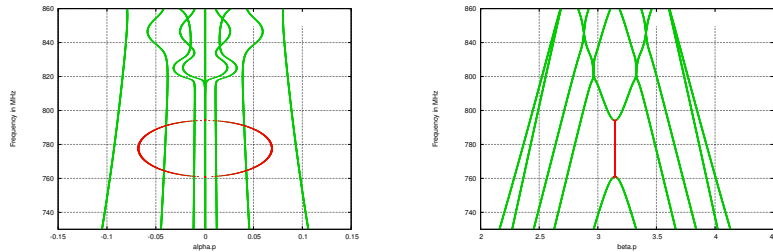
Fig. 10. Dispersion context of piezoelectric structure with periodic arranged electrodes

the stop-band of the chosen filter structure. On the left the context between

the frequency and the attenuation-constant α per cell is drawn, while on the right the context between frequency and phase shift β in each cell. Above the upper stop-band edge we can observe an increased attenuation caused by bulk wave radiation, which is enabled by absorbing boundary conditions at the bottom and does not occur in simulations including only standard boundary conditions.

7 Conclusions

We gave a full detailed modeling for piezoelectric surface acoustic wave filters. We started with developing mathematical tools for periodic structures for the scalar wave equation. In order to reduce the computation domain while allowing wave absorption we introduced absorbing boundary conditions at the artificial bottom boundary. By an abstract formulation we achieved that the developed methods are directly applicable on the piezoelectric field equations. With the Inner-Node-Matrix and the Schur-Complement method we provided and implemented two solution strategies. The Schur-Complement method is suitable for solving the dispersion context for the three dimensional piezoelectric equations with an underlying two dimensional geometry strategy. However, if one wants to extend the model to 3 dimensional geometries, iterative algorithms using only matrix-vector products are recommendable. This is provided by the Inner-Node-Matrix method.

Another possible model improvement would be gained by perfectly matched layers which allow an improved wave absorption into the material. We showed that the introduced methods are still applicable in such models.

The developed algorithms can be also applied to other problem fields including periodic structures like Maxwell's equations for simulating photonic crystals. By numerical experiments we compared the dispersion diagrams of homogenous versus periodic structures and observed the classification of the frequency domain into pass- and stop-band in the later one. Finally, we simulated a piezoelectric structure as used for frequency filtering in common TV-sets.

References

1. E. Anderson, Z. Bai, C. Bischof, J. Demmel, J. Dongarra, J. Du Croz, A. Greenbaum, S. Hammarling, A. McKenney, S. Ostrouchov, and D. Sorensen. *LAPACK Users' Guide*. SIAM, Philadelphia, third edition, 1999.
2. Mermin Ashcroft. *Solid State Physics*. Holt-Sounders International, 1976.
3. B. Auld. *Acoustic Fields and Waves in Solids*, volume 1,2. Krieger, second edition, 1990.
4. W. Axmann and Kuchment P. An efficient finite element method for computing spectra of photonic and acoustic band-gap materials, scalar case. *Journal of Computational Physics*, 150:468–481, 1999.
5. Z. Bai, J. Demmel, J. Dongarra, A. Ruhe, and H. van der Vorst, editors. *Templates for the solution of Algebraic Eigenvalue Problems: A Practical Guide*. SIAM, Philadelphia, 2000.
6. A. Bensoussan, J.L. Lions, and G. Papanicolaou. High frequenca wave propagation in periodic structures. In J. L. Lions, G. Papanicolaou, and R.T. Rockafellar, editors, *Asymptotic Analysis for periodic structures*, Studies in Mathematics and its Applications, pages 614–626. North-Holland, 1978. Section 3, Spectral theroy of differential operators with periodic coefficients.
7. C. Bernardi, Y. Maday, , and A. Patera. A new nonconforming approach to domain decomposition: the mortar element method. *Nonlinear partial differential equations and their applications (1994)*, pages 13–51, 1994.
8. B. Bunse-Gerstner, R. Byers, and V. Mehrmann. A chart on numerical methods for structured eigenvalue problems. *SIAM Journal of Matrix Analysis and its Applications*, 13:419–453, 1992.
9. F.M. Gomes and D.C. Sorensen. ARPACK++: a C++ implementation of arpack eigenvalue package. Technical report, Computational and Applied Mathematics, Rice University, 1997.
10. M. Hofer, N. Finger, S. Zaglmayr, J. Schöberl, G. Kovacs, U. Langer, and R. Lerch. Finite element calculation of the dispersion relations of infinitely extended saw structures , including bulk wave radiation. In Vittal S. Rao, editor, *Proceedings of SPIE's 9th Annual International Symposium on Smart Structures and Materials*, pages 472–483. SPIE, 2002.
11. M. Hofer, N. Finger, S. Zaglmayr, J. Schöberl, G. Kovacs, U. Langer, and R. Lerch. Finite element calculation of wave propagation and excitation in periodic piezoelectric systems. In *Proceedng of the Fifth World Congress on Computational Mechanics (WCCM V)*. Vienna University of Technology, Austria, 2002.
12. M. Koshiba, S. Mitobe, and M. Suzuki. Finite-element solution of periodic waveguides for acoustic waves. *IEEE Transactions on Ultrasonics, Ferroelectrics and Frequency Control*, 34(4), 1987.
13. P. Kuchment. *Floquet theory of partial differential equations*, volume 60 of *Operator Theory Advances and Applications*. Birkhaeuser Verlag, Basel and Boston, 1993.
14. R.B. Lehoucq, D.C. Sorensen, and C. Yang. ARPACK users' guide: Solution of large scale eigenvalue problems with implicitly restarted arnoldi methods. Technical report, Computational and Applied Mathematics, Rice University, 1997.

15. R. Lerch. Analyse hochfrequenter akustischer Felder in Oberflächenwellenfilter-Komponenten. *Archiv für elektronische Übertragungstechnik (AEU)*, 44(4):317–327, 1990.
16. R. Lerch. Simulation of Piezoelectric Devices by Two- and Three-Dimensional Finite Elements. *IEEE Transactions on Ultrasonics, Ferroelectrics and Frequency Control*, 37(3):233–247, 1990.
17. O. Madelung. *Grundlagen der Halbleiterphysik*, chapter 12. Folgerungen aus der Translationsinvarianz. Springer, Berlin, 1970.
18. V. Mehrmann and D. Watkins. Structure-preserving methods for computing eigenpairs of large sparse skew-hamiltonian/hamiltonian pencils. *SIAM J. Sci. Comput.*, 22(6):1905, 2001.
19. D.P. Morgan. History of SAW Devices. In *IEEE Frequency Control Symposium*, pages 439–460, 1998.
20. N. Reed and B. Simon. *Analysis of Operators*, volume 4 of *Methods of Modern Mathematical Physics*, chapter 13 Spectral Analysis. Academic Press, 1978.
21. J. Schöberl. Netgen - an advancing front 2d/3d-mesh generator based on abstract rules. *Comput.Visual.Sci*, (1):41–52, 1997.
22. J. Schöberl. Ngsolve. Online manual, 2003. www.hpfem.jku.at.
23. F. Tisseur and K. Meerbergen. The quadratic eigenvalue problem. *SIAM Review*, 43(2):235–286, 2001.
24. B. Wohlmuth. A mortar finite element method using dual spaces for the Lagrange multiplier. *SIAM Journal on Numerical Analysis*, 38(3):989–1012, 2001.
25. S. Zaglmayr. Eigenvalue problems in surface acoustic wave filter simulations. Master's thesis, Institute of Computational Mathematics, Johannes Kepler University Linz, Austria, 2002.